

Complementary Self-Aligned
Graded-Barrier Quantum-Well Laser
 $L_z = 30 \text{ \AA}$
Length = 356 μm
Width = 9 μm
Pulsed Photodiode Response

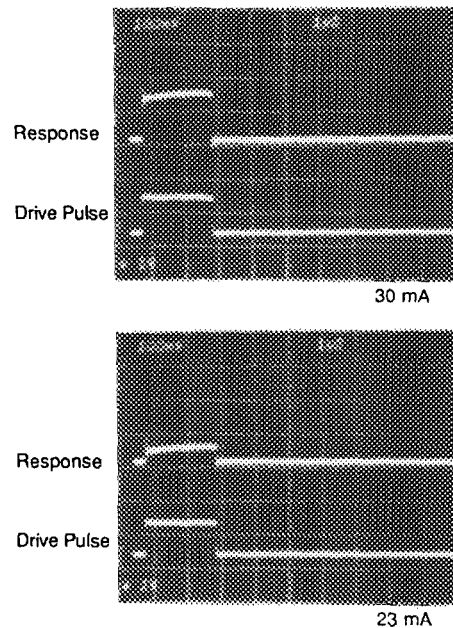


FIG. 5. Pulsed photodiode response of a real index-guided complementary self-aligned graded barrier quantum well laser. No lasing delay or transient behavior above threshold is observed in these devices.

ide defined stripe geometry graded barrier quantum well laser diodes by observing the near- and far-field patterns at different drive pulse widths. Also, low threshold devices have been fabricated with built-in index steps along the junction plane eliminating the long lasing delay and transient behavior associated with thermally induced index guiding. Stable mode behavior is observed in these devices up to 15 mW per uncoated facet.

The authors would like to thank Y. S. Moroz, B. K. Moroz, C. W. Trussel, and P. D. Dapkus for their contributions to this work. This work was supported in part by U.S. Army Night Vision Laboratory contract DAAK 20-84-K-0225 and U.S. Army Research Office contract DAAG 29-85-G-0133.

¹W. T. Tsang, *Appl. Phys. Lett.* **40**, 217 (1982).

²P. S. Zory, A. R. Reisinger, L. J. Mawst, G. Costrini, C. A. Zmudzinski, M. A. Emanuel, M. E. Givens, and J. J. Coleman, *Electron. Lett.* **22**, 475 (1986).

³P. S. Zory, A. R. Reisinger, R. G. Waters, L. J. Mawst, C. A. Zmudzinski, M. A. Emanuel, M. E. Givens, and J. J. Coleman, *Appl. Phys. Lett.* **49**, 16 (1986).

⁴F. C. Prince, N. B. Patel, D. Kasemset, and C. S. Hong, *Electron. Lett.* **19**, 435 (1983).

⁵F. C. Prince, T. J. S. Mattos, N. B. Patel, D. Kasemset, and C. S. Hong, *IEEE J. Quantum Electron.* **QE-21**, 634 (1985).

⁶L. J. Mawst, G. Costrini, C. A. Zmudzinski, M. E. Givens, M. A. Emanuel, and J. J. Coleman, *Electron. Lett.* **21**, 903 (1985).

⁷G. P. Agrawal, *IEEE J. Lightwave Tech.* **LT-2**, 537 (1984).

⁸R. D. Burnham, C. Lindstrom, T. L. Paoli, D. R. Scifres, W. Streifer, and N. Holonyak, Jr., *Appl. Phys. Lett.* **42**, 937 (1983).

Correlation between the cohesive energy and the onset of radiation-enhanced diffusion in ion mixing

Y.-T. Cheng, X.-A. Zhao,^{a)} T. Banwell, T. W. Workman, M.-A. Nicolet, and W. L. Johnson

California Institute of Technology, Pasadena, California 91125

(Received 28 April 1986; accepted for publication 7 July 1986)

A correlation between the cohesive energy of elemental solids and the characteristic temperature T_c for the onset of radiation-enhanced diffusion during ion mixing is established. This correlation enables one to predict the onset of radiation-enhanced diffusion for systems which have not yet been investigated. A theoretical argument based on the current models of cascade mixing and radiation-enhanced diffusion is provided as a basis for understanding this observation.

The phenomenon of atomic mixing of thin layers by ion beam irradiation has been the subject of numerous studies.¹ Several models have been proposed to account for the observed mixing phenomena. It is now generally accepted that collisional cascade² and thermal-spike effects³ are the primary factors which influence the mixing induced by energetic heavy ions at "low" ambient temperatures, whereas at "high" ambient temperatures, radiation-enhanced diffusion

^{a)} Permanent address: Shanghai Institute of Metallurgy, Academy of Sciences of China, Shanghai, People's Republic of China.

plays a dominant role.⁴ There exists a narrow temperature range which separates the temperature-independent or low-temperature ion mixing from the Arrhenius-type radiation-enhanced diffusion region, and this serves as a basis for defining a critical temperature T_c . In this communication, we establish a correlation between T_c and the average cohesive energy of elemental solids which are mixed. This correlation thus enables one to predict the onset of radiation-enhanced diffusion (T_c) for systems which have not yet been investigated.

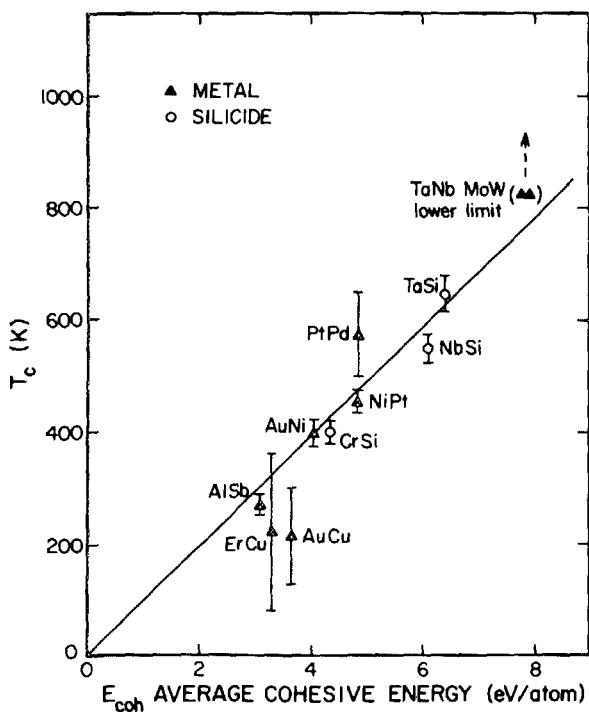


FIG. 1. Correlation between the cohesive energy of the system and the critical temperature T_c at which radiation-enhanced diffusion becomes dominant. TaSi, Ref. 9; NbSi, Ref. 10; NiPt, and AuNi, Ref. 11; CrSi, Ref. 12; AuCu, Ref. 13; AISb, Ref. 14; ErCu, Ref. 15.

The systems we have studied are W-Mo, Ta-Nb, and Pt-Pd bilayers. The metals used have relatively high cohesive energies,⁵ but each binary couple has nearly zero heats of mixing.⁶ Therefore, we are able to isolate the effect of cohesive energy from the possible influence of a chemical driving force on radiation-enhanced diffusion. Furthermore, all the 5d (and 4d) elements have nearly the same atomic number and mass, while the mass difference between the top (5d) and bottom (4d) layer of each couple is sufficient to resolve their $^4\text{He}^+$ backscattering signals and study the intermixing process by backscattering spectrometry.⁷

Thin bilayer samples were prepared by *e*-gun evaporation in an oil-free vacuum system at a pressure of less than 8×10^{-8} Torr during evaporation. All bilayers consisted of a layer of 5d element on top of a ~ 200 -nm-thick layer of 4d element sequentially deposited onto a SiO_2 substrate. The top layer thickness was adjusted to 90% of the projected range of 600-keV Xe^{++} ions. Ion mixing was performed to a dose of $5 \times 10^{15}/\text{cm}^2$, using 600-keV Xe^{++} , at substrate temperatures of 300, 520, 630, 720, and 800 K (the highest accessible temperature of our instrument). Samples of all three types were irradiated simultaneously at each specified temperature. Backscattering analysis was performed with 2-MeV He^+ ions incident at an angle of 30° against the sample normal and a scattering angle of 170° in the plane of the beam and the rotation axis of the sample.

The backscattering spectra were analyzed by a fitting routine described in a previous paper.⁸ Within our experimental resolution, there was no noticeable change in the amount of mixing for Ta-Nb and W-Mo bilayers when the

substrate temperature varied from 300 to 800 K. This upper temperature thus represents the lower bound on T_c for the Ta-Nb and W-Mo systems. A substantial increase in the rate of mixing was detected in the Pt-Pd system as the temperature was varied from 520 to 630 K.

Additional data concerning the temperature dependence of ion mixing were obtained from the literature.⁹⁻¹⁶ In Fig. 1, we plot T_c versus the average cohesive energy E_{coh} for a variety of systems. E_{coh} is the arithmetic average of the cohesive energies of the pure elements in each binary system.⁵ T_c is defined by the intersection of the high- and low-temperature asymptotes or the temperature range where a substantial increase in the rate of mixing was reported. The error bars in some cases were taken to be the temperature steps of the experiment where radiation-enhanced diffusion was observed. The Ni-Si system exhibits a very wide transition from the low- to high-temperature region.¹⁸ T_c is therefore not well defined, and this system is not included in Fig. 1.

A correlation between T_c and E_{coh} as shown in Fig. 1 is apparent. The greater the average cohesive energy of the component layers E_{coh} , the higher is the critical ambient temperature T_c , where radiation-enhanced diffusion becomes dominant. Since data in Fig. 1 come from many sources and each ion mixing experiment was performed with different ion, energy, dose, and dose rate, we conclude that these parameters are of minor importance compared to the cohesive energy of the system irradiated. Furthermore, the relationship between T_c and E_{coh} is roughly linear as shown in Fig. 1. All these features may be explained by the following argument.

Phenomenologically, we can describe the behavior of the amount of mixing versus $1/T$ by an effective diffusion coefficient of the form

$$D = D_c + D_r e^{-Q/K_B T}. \quad (1)$$

The first term on the right-hand side is temperature independent, and the second term has an Arrhenius-type temperature dependence, where Q is an apparent activation energy. The first term on the right dominates at low temperatures (cascade mixing), whereas the second term dominates at high temperatures (radiation-enhanced diffusion).

At a temperature near T_c , the two terms on the right of Eq. (1) contribute equally and

$$T_c = (1/K_B) [\ln(D_r/D_c)]^{-1} Q. \quad (2)$$

Now, let us assume that there is a scaling relationship between the apparent activation energy (Q) and the cohesive energy of the matrix (E_{coh}), i.e., $Q = S E_{coh}$, where S is a constant. This kind of scaling relationship is known to exist in vacancy diffusion in single elements.^{17,18} We then obtain

$$T_c = (S/K_B) [\ln(D_r/D_c)]^{-1} E_{coh}. \quad (3)$$

The linear relationship between T_c and E_{coh} is obtained provided that the logarithmic function varies slowly with its argument. In concept, D_c may be calculated using cascade mixing, or thermal spike models.^{2,3} D_r can be obtained from radiation-enhanced diffusion models.^{19,20} We estimated the logarithmic term $\ln(D_r/D_c)$ for several systems for which the necessary parameters were readily available (please see

TABLE I. Numerical estimation of $\ln(D_r/D_c)$.

System	MoW	AlSb	AuCu	CrSi	NiPt	NiAu
$D_0(\text{cm}^2/\text{s})^a$	$4 \times 10^{-2}{}^b$	$9 \times 10^{-2}{}^c$	$2.36 \times 10^{-6}{}^d$	$10^{-2}{}^e$	$2.6 \times 10^{-9}{}^f$	$1.4 \times 10^{-7}{}^f$
$E_d(\text{eV})^g$	40	16.5(Al)	28	21	30	30
$(dE/dX)_n(\text{eV}/\text{\AA})^h$	500(Xe ⁺⁺)	35(Ar ⁺)	280(Kr ⁺)	350(Xe ⁺)	570(Xe ⁺)	550(Xe ⁺)
D_r/D_c^i	2.8×10^6	10 ⁷	2.2×10^4	1.2×10^6	5.7×10^2	4.3×10^3
$\ln(D_r/D_c)$	15	16	10	14	6.3	8.4

^a Frequency factor D_0 of thermal-diffusion coefficient.

^b *Diffusion Data*, edited by F. H. Wöhlbier, Vol. 6 (Trans Tech S.A., Aademansdorf, Switzerland, 1972), p. 206.

^c A. D. LeClaire, *J. Nucl. Mater.* **69/70** (1978), p. 71.

^d *Diffusion Data*, Vol. 12, edited by F. H. Wöhlbier (Trans Tech S.A., Aademansdorf, Switzerland, 1976), p. 233.

^e *Diffusion Data*, Vol. 4, edited by F. H. Wöhlbier (Trans Tech S.A., Aademansdorf, Switzerland, 1970), p. 415.

^f *Diffusion Data*, Vol. 35, edited by F. H. Wöhlbier (Trans Tech S.A., Aademansdorf, Switzerland, 1984), p. 165.

^g Average displacement energy $E_d = (E_A + E_B)/2$ for each A-B system. E_A and E_B are obtained from H. H. Anderson, *Appl. Phys.* **18**, (1979), p. 131.

^h Energy deposited per unit path length due to nuclear collision, estimated from J. P. Biersach and J. F. Ziegler, *Ion Implantation Techniques*, edited by H. Ryssel and H. Glawisching (Springer, Berlin, 1982), p. 122.

$$i \frac{D_r}{D_c} = \frac{6}{\lambda^2} \left(\frac{2}{0.8\pi} \right)^{1/2} \left(\frac{\alpha D_0 E_d}{R_{iw} (dE/dX)_n \phi} \right)^{1/2},$$

where $\lambda^2 \sim 100 \text{\AA}^2$, $\alpha \sim 0.025$, $R_{iw} \sim 10 \text{\AA}$, $\phi \sim 3 \times 10^{13} \text{ ion/cm}^2 \text{ s} \sim 3 \times 10^{-3} \text{ ion/\AA}^2 \text{ s}$ (see Ref. 20).

Table I). Despite the fact that the factor (D_r/D_c) varies by four orders of magnitude, the logarithmic term remains within 47% from its mean value $[\ln(D_r/D_c)]_{\text{ave}} = 11.6$. From the estimated slope of the line in Fig. 1 ($\sim 100 \text{ K/eV}$), and $[\ln(D_r/D_c)]_{\text{ave}}$, we obtain $S \sim 0.1$, i.e., $Q \sim 0.1 E_{\text{coh}}$ from Eq. (3).

Using the scaling relationship for the vacancy migration energy $E_v^m = 0.24 E_{\text{coh}}$,¹⁷ together with a proposed model for radiation-enhanced diffusion in which the activation energy is half of the vacancy migration energy,^{19,20} we obtain $Q \sim 0.12 E_{\text{coh}}$. Thus, we conclude that our experimental observation and theoretical interpretation are consistent with a picture of radiation-enhanced diffusion due to vacancy migration. A similar conclusion has also been reached from a different approach.²¹

A remarkable feature of this correlation is that it includes both metal-metal and metal-silicon systems. For both cases, the mixed layer is metallic. Furthermore, the correlation is structure independent. The mixed layers can be metallic solid solutions (e.g., Pt-Ni), metallic compounds (e.g., Co₂Si), or amorphous metallic alloys (e.g., Cu-Er). We believe that for the case of metallic systems, the formation and migration enthalpies of vacancies (holes in the case of amorphous material) are determined mainly by the local atomic environment and corresponding interaction potentials and not by the long-range order of the system.

In summary, we have demonstrated a correlation between the cohesive energy of the system and the characteristic temperature range for the onset of radiation-enhanced diffusion. A simple argument based on the current models of cascade mixing (or thermal spikes) and radiation-enhanced diffusion provides a basis for understanding this observed correlation. Both the experimental observation and the theoretical interpretation are consistent with a model based on a vacancy mechanism for radiation-enhanced diffusion. We view the experimentally observed correlation between T_c and cohesive energy, and the theoretical arguments, as valid only to a lowest-order approximation. Further investigations on the influence of the ion irradiation parameters (en-

ergy, dose, dose rate), and the structure of the matrix will be required for a more critical evaluation of the dependence of T_c on E_{coh} .

The authors would like to thank Mr. D. Groseth for sample preparation and Dr. M. Van Rossum for helpful discussions. This work is supported by the National Science Foundation under Grant No. DMR-8421119.

¹B. M. Paine and R. S. Averback, *Nucl. Instrum. Methods B* **7/8**, 666 (1985).

²P. Sigmund and Gras-Marti, *Nucl. Instrum. Methods* **182/183**, 25 (1981).

³W. L. Johnson, Y.-T. Cheng, M. Van Rossum, and M.-A. Nicolet, *Nucl. Instrum. Methods B* **7/8**, 657 (1985).

⁴S. Matteson, J. Roth, and M.-A. Nicolet, *Radiat. Eff.* **42**, 217 (1979).

⁵C. Kittel, *Introduction to Solid State Physics* (Wiley, New York, 1976), p. 74.

⁶A. R. Miedema, *Philips Tech. Rev.* **8**, 36 (1976).

⁷W. K. Chu, J. W. Mayer, and M.-A. Nicolet, *Backscattering Spectrometry* (Academic, New York, 1978).

⁸Y.-T. Cheng, M. Van Rossum, M.-A. Nicolet, and W. L. Johnson, *Appl. Phys. Lett.* **45**, 185 (1984).

⁹F. So (private communication).

¹⁰S. Matteson, J. Roth, and M.-A. Nicolet, *Radiat. Eff.* **42**, 217 (1979).

¹¹J. Bottiger, S. K. Nielsen, and P. T. Thorsen, in *Amorphous Metals and Non-Equilibrium Processing*, edited by M. Von Allmen (Les Editions de Physique, Les Ulis Cedex, 1984), p. 111.

¹²J. W. Mayer, B. Y. Tsaur, S. S. Lau, and L. S. Hung, *Nucl. Instrum. Methods* **182/183**, 1 (1981).

¹³Z. L. Wang, J. F. M. Westendorp, S. Doorn, and F. W. Saris, in *Metastable Materials Formation by Ion Implantation*, edited by S. T. Picraux and W. J. Choyke (Elsevier, New York, 1982), p. 59.

¹⁴B. Paine, M.-A. Nicolet, and T. Banwell, in *Metastable Materials Formation by Ion Implantation*, edited by S. T. Picraux and W. J. Choyke (Elsevier, New York, 1982), p. 79.

¹⁵H. Hahn, R. S. Averback, T. de la Rubia, and P. R. Okamoto, in *Beam-Solid Interactions and Phase Transformations*, edited by H. Kurz, G. L. Olsen, and J. M. Poate (Materials Research Society, Pittsburgh, PA, 1986), p. 491.

¹⁶L. S. Wielunski, B. M. Paine, B. X. Liu, C.-D. Lien, and M.-A. Nicolet, *Phys. Status Solidi A* **72**, 399 (1982).

¹⁷M. Doyama, and J. S. Koehler, *Acta Metall.* **24**, 871 (1976).

¹⁸G. P. Tiwari, in *Materials Science Forum*, Vol. 1, edited by G. E. Murch (Trans Tech, Aademansdorf, 1984), p. 171.

¹⁹G. J. Dienes and A. C. Damask, *J. Appl. Phys.* **29**, 1713 (1958).

²⁰S. M. Myers, *Nucl. Instrum. Methods* **168**, 265 (1980).

²¹R. S. Averback and D. Peak, *Appl. Phys. A* **38**, 139 (1985).